ARTICLE

Rheological properties of HDPE/chitosan composites modified with PE-*g*-MA

Poliana S. Lima, Rebecca S.F. Brito, Bárbara F.F. Santos, Albaniza A. Tavares, Pankaj Agrawal, and Daniela L.A.C.S. Andrade
Department of Materials Engineering, Federal University of Campina Grande, Campina Grande, PB 58429-900, Brazil

Renate M.R. Wellen
Department of Materials Engineering, Federal University of Paraíba, João Pessoa, PB 58051-900, Brazil

Eduardo L. Canedo and Suédina M.L. Silva[a)]
Department of Materials Engineering, Federal University of Campina Grande, Campina Grande, PB 58429-900, Brazil

(Received 24 August 2016; accepted 19 December 2016)

The rheological behavior of composites made with high-density polyethylene (HDPE) and chitosan was studied. Composites were prepared by melt processing in a laboratory internal mixer. Maleic anhydride grafted HDPE (PE-*g*-MA) was used as compatibilizer to enhance the dispersion of chitosan in the HDPE matrix. Different percentages of chitosan and compatibilizer (up to a maximum of 25 phr) were added into HDPE to prepare composites. Characterization of the composites with parallel plate rheometer and laboratory internal mixer revealed that the presence of chitosan increases the complex viscosity, loss modulus, storage modulus and the torque (i.e., melt viscosity), and the combination chitosan/compatibilizer has a similar, if slighter, effect. At higher filler levels it is clear that the PE-*g*-MA affected the microstructure of the compounds, possibly increasing matrix–filler interactions and acting as an effective compatibilizer.

I. INTRODUCTION

High density polyethylene (HDPE) is a versatile material that offers a high cost/benefit ratio compared to other polymers and alternative materials such as glass, metal or paper. It is widely used in high volume for short term applications such as biaxially oriented films for packaging, blown molded bottles for food, carrier bags, food wrapping material and so on.[1–3] Although HDPE can offer a combination of characteristics that are ideally suited to various applications, such as good flow, good thermal stability, and excellent chemical resistance, this polymer decompose after long periods of time in natural environments; so, it is a source of pollution and social concern when disposed as solid waste.[4–9] Still, HDPE packaging has poor antimicrobial and antifungal activities and little bivalent metal chelating ability.[2,3,10–13]

The incorporation of fillers from renewable resources as functional additives (such as chitosan, starch, cellulose and their derivatives) into synthetic polymers, has been reported in many publications and has been considered one of the best routes for preparing new materials with useful properties, partially or totally biodegradable.[14–24]

Chitosan is a natural polyaminosaccharide, composed by *N*-acetyl-D-glucosamine and *D*-glucosamine units linked by β glycosidic bonds. It is obtained from the deacetylation of chitin, one of the world's most plentiful, renewable organic resources (a major constituent of the shells of crustaceans, the exoskeletons of insects and the cell walls of fungi), and has a great potential as filler. This is due to its biodegradability, biocompatibility, antimicrobial activity, non-toxicity and versatile chemical and physical properties.[25–32] Moreover, chitosan is obtained at a relatively low cost and it is eco-friendly, safe for humans and for the environment.[28,33,34]

In view of the above mentioned considerations, the development of research about polyethylene/chitosan composites has received considerable attention, especially those prepared by melt processing, because of their high yield, and greater control of the final material's characteristics without atmospheric pollution, in comparison with the solvent evaporation methods.[12,14,15,35–49] However, there are only a few published reports on polyethylene/chitosan composites rheological characteristics.[38,46]

In this work, the rheological behavior of composites made with HDPE and chitosan was studied. The composites were prepared by using a melt compounding

Contributing Editor: Sarah Morgan
[a)]Address all correspondence to this author.
e-mail: suedina.silva@ufcg.edu.br
DOI: 10.1557/jmr.2016.519

processing in a laboratory internal mixer. Maleic anhydride grafted HDPE was used as compatibilizer to enhance the dispersing effect of chitosan in the HDPE matrix. Different percentages of chitosan and compatibilizer (up to a maximum of 25 phr) were added into HDPE for preparing samples. The thermal and mechanical properties of these composites were evaluated and reported elsewhere.[50]

II. EXPERIMENTAL

A. Materials

The high density polyethylene (HDPE), injection molding grade JV060U supplied by Braskem (São Paulo, Brazil), is a 1-butene copolymer of narrow molecular weight. It contains antioxidants and UV stabilizer additives. It has a density of 0.957 g/cm^3 (ASTM D 792) and a melt index of 7 dg/min (ASTM D1238, 190 °C/2.16 kg).[51] Density of HDPE at processing temperature (about 190 °C) was estimate in 0.76 g/cm^3.[52] The chitosan used in this work is powder supplied by Polymar (Fortaleza, Brazil), has a 86.7% nominal degree of deacetylation. True density of chitosan was estimated as 1.48 g/cm^3 at processing conditions.[53–55] Maleated polyethylene (PE-*g*-MA), Polybond 3009 from Chemtura (São Paulo, Brazil), a grafted linear polyethylene with 1% maleic anhydride content and melt index of 6 dg/min, was used as compatibilizer in HDPE/chitosan compounds.[56]

Chitosan particle size distribution was measured (in triplicate) by light scattering in a Nanoparticle Analyzer SZ-100 (Horiba Scientific, Stanmore, United Kingdom), in a dispersion of chitosan powder (as received) in dilute acetic acid. Typical results are shown in Fig. 1. Weight-average particle diameter was 50 nm, with 95% of the material under 150 nm.

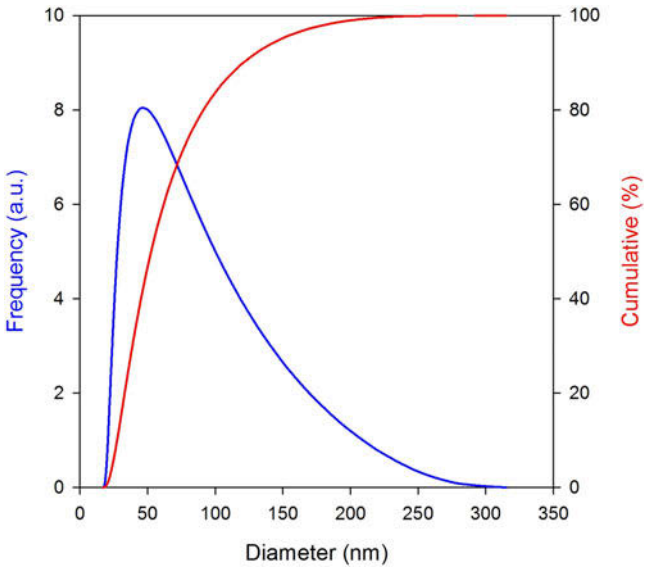

FIG. 1. Particle size distribution of chitosan.

B. Preparation of HDPE/chitosan compounds

HDPE/chitosan compounds were prepared in a Haake Rheomix 3000 laboratory internal mixer (Thermo Fisher Scientific, Frankfurt, Germany) fitted with high intensity rotors (roller type) operated at 60 rpm with the chamber wall maintained at 180 °C. Batch mass was selected to fill 90% of the processing chamber volume during the last stage of the process (fully molten material). HDPE (as received) with and without PE-*g*-MA compatibilizer (dried under vacuum for 24 h at 80 °C) was loaded first. After 6 min, chitosan (dried under the same conditions) was added without interrupting the process. Mixing continued for another 4 min. HDPE/chitosan compounds were removed, dried at room temperature, ground, and stored in sealed containers. Sample compositions prepared are summarized in Table I. PE-*g*-MA and chitosan were coded as C and Q, respectively.

C. Rheological characterization

A parallel plate rheometer Anton Parr Physica MCR 301 (Anton Parr GmbH, Graz, Austria), with a plate diameter of 25 mm and a 1 mm gap was run in small amplitude oscillatory mode to measure the rheological properties of selected processed samples. Tests were conducted at 180, 200 and 220 °C and frequencies between 1 and 100 s^{-1}. Results were used to estimate the shear viscosity and elastic characteristics of the molten materials as functions of shear rate and temperature.

Torque (Z) and internal temperature (T) as functions of time (t), registered by the mixer at 1 s intervals were used to estimate the dependence of the viscosity on filler

TABLE I. Formulation of the prepared samples.

Code	Matrix (wt%)		Chitosan (phr)
	HDPE	PE-*g*-MA	
HDPE	100	0	0
HDPE/C5	95	5	0
HDPE/C10	90	10	0
HDPE/C15	85	15	0
HDPE/C20	80	20	0
HDPE/C25	75	25	0
HDPE/Q5	95	0	5
HDPE/Q10	90	0	10
HDPE/Q15	85	0	15
HDPE/Q20	80	0	20
HDPE/Q25	75	0	25
HDPE/C5/Q5	95	5	5
HDPE/C10/Q10	90	10	10
HDPE/C15/Q15	85	15	15
HDPE/C20/Q20	80	20	20
HDPE/C25/Q25	75	25	25

content in samples with and without compatibilization. Processability of the system at tested conditions was discussed.

D. Thermogravimetry (TG)

Thermogravimetric analysis was performed in a Shimadzu TGA S1HA instrument (Shimdazu Corp., Kyoto, Japan). Samples of approximately 5 mg in open alumina crucibles were heated from 30 °C to 800 °C at 10 °C/min in a flow of 50 mL/min of nitrogen gas; sample mass and temperature were recorded as function of time.

E. Scanning electron microscopy (SEM)

SEM images were captured in a Shimadzu SXX-550 instrument (Shimadzu Corp.) on film samples fractured in liquid nitrogen. A fine layer of gold was deposited over the fracture surfaces prior to test.

III. RESULTS AND DISCUSSION

A. Thermogravimetric analysis (TGA)

Figure 2 shows TGA plots of chitosan, HDPE/PE-*g*-MA blends, and HDPE/chitosan compounds with and without compatibilizer. After an initial stage at 26–150 °C, probably associated with the loss of free water (dehumidification), neat chitosan [Fig. 2(a)] losses 45% weight in a second step at a mean temperature of 295 °C, which may be attributed to deacetylation and early stages of degradation of the polymer.[38,57] HDPE and PE-*g*-MA [Fig. 2(b)] show a sharp and complete degradation a mean

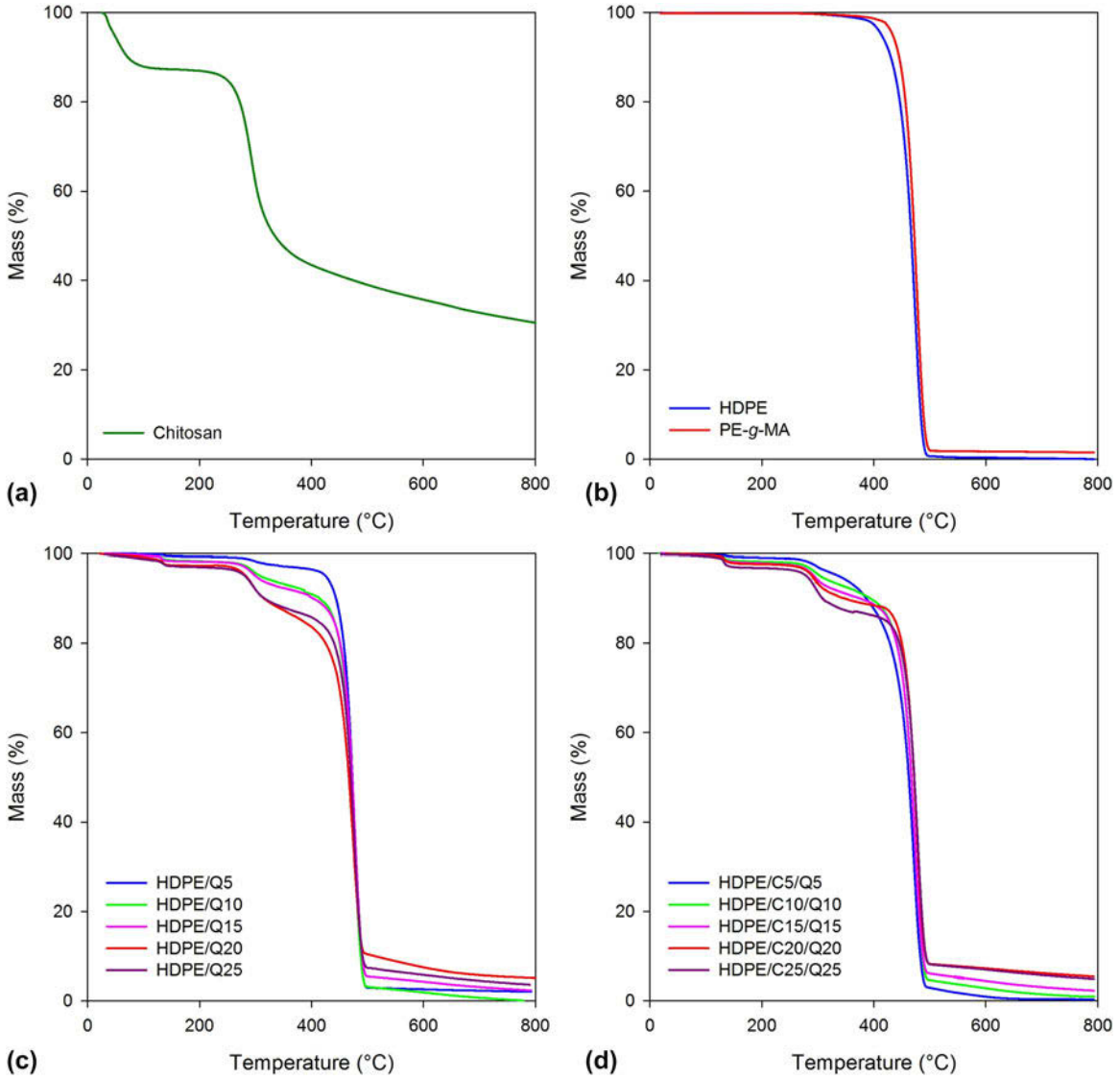

FIG. 2. Thermogravimetric results for chitosan (a), HDPE and PE-*g*-MA (b), and HDPE/chitosan compounds without (c) and with (d) PE-*g*-MA compatibilizer.

temperature of 470 °C. Compounds [Figs. 2(c) and 2(d)] show both: deacetylation/degradation of the chitosan (centered at 295 °C) in proportion to the load content, and complete degradation of the matrix at 470 °C. We conclude that under the rheological testing conditions (up to 200 °C) chitosan is thermally stable.

B. Parallel plate rheometry

Samples of HDPE, the blend HDPE/25% PE-*g*-MA, and HDPE/chitosan compounds with 25% filler, with and without compatibilization, were tested in oscillatory mode on a parallel plate rheometer, according to the procedure described in the previous section. Tests were conducted at 180 °C, 200 °C, and 220 °C at low amplitude (4 miliradians for the polymers, between 0.4 e 0.08 miliradians for the compounds), within the linear viscoelastic regime for frequencies studied. Figure 3 shows the elastic moduli in shear, in phase with the deformation (storage modulus G') and out of phase (loss modulus G'').

Moduli increase with frequency (ω), with the loss modulus greater than the storage modulus ($G' < G''$) for all frequencies and temperatures studied. However, they converge at high frequencies, suggesting a crossover point at $\omega > 100\ s^{-1}$. The presence of filler increases the moduli, and the compatibilizer has a similar, if slighter, effect.

The absolute value of the complex viscosity was computed as:

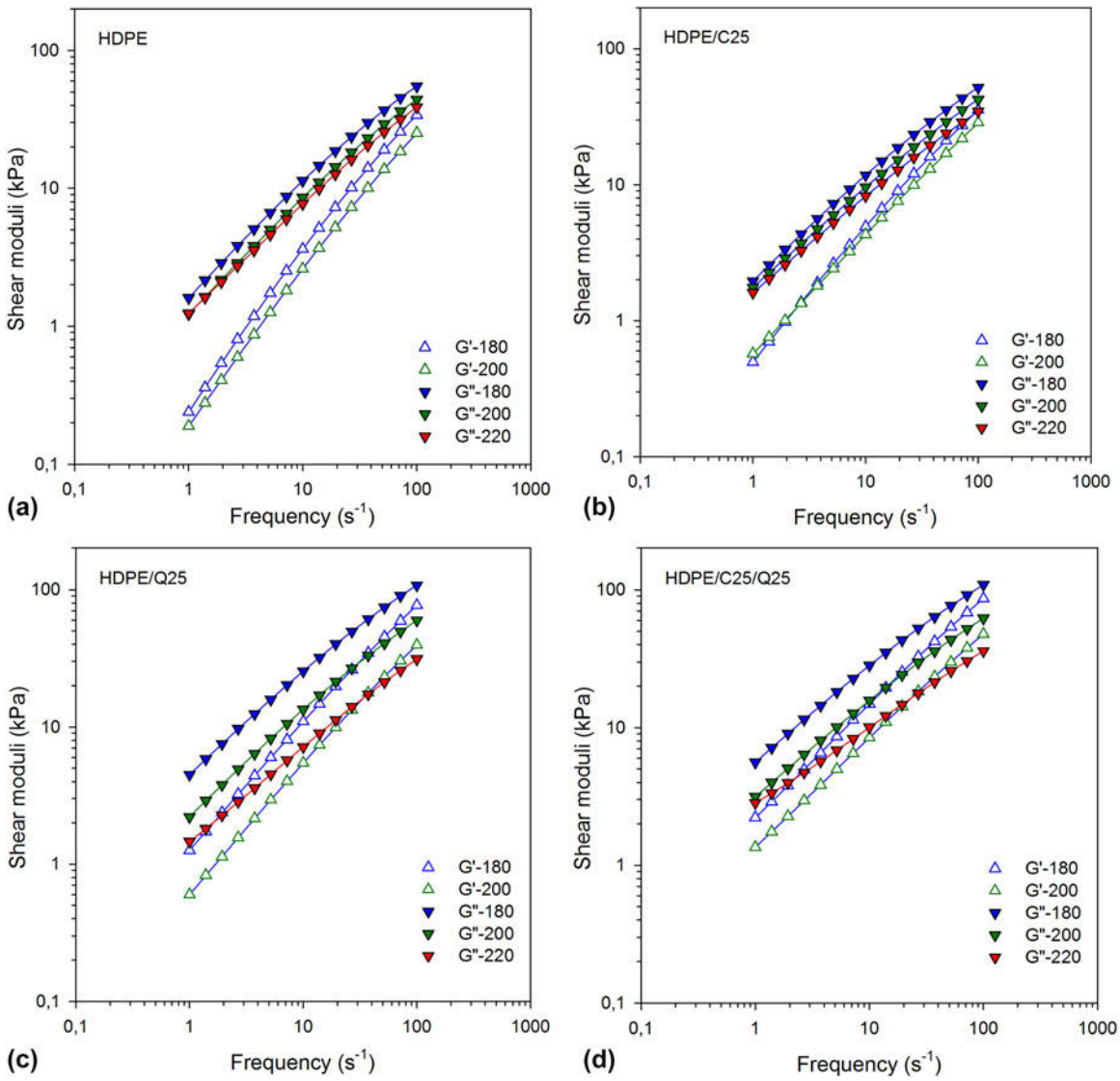

FIG. 3. Storage (G') and loss (G'') shear moduli as functions of frequency at several temperatures, for neat HDPE (a), HDPE/25% PE-*g*-MA blend (b), and HDPE/chitosan compounds with 25% filler, without compatibilization (c) and with 25% PE-*g*-MA compatibilizer (d). Logarithmic scales.

$$|\eta^*| = \frac{\left(G'^2 + G''^2\right)^{1/2}}{\omega} \quad . \tag{1}$$

The empirical Cox–Merz rule[58] allows the estimate of the ordinary (shear) viscosity as a function of the shear rate:

$$\eta(\dot{\gamma}) = |\eta^*(\omega)|_{\omega=\dot{\gamma}} \quad . \tag{2}$$

Cox–Merz rule has been extensively discussed and periodically reconsidered in the rheological literature.[59,60] The rule appears to be applicable to concentrated suspensions under the conditions tested in the present work.[61] Viscosities estimated according to Eqs. (1)–(2) are shown in Fig. 4.

The molten materials behave as pseudoplastics in the range tested. HDPE and the blend HDPE/PE-*g*-MA are in intermediate zone between Newtonian and non-Newtonian regimes; filled compounds are virtually in the power-law zone. In the first case, viscosity as a function of shear rate and temperature may be correlated using the Cross model:[62,63]

$$\eta(\dot{\gamma}, T) = \frac{\eta_0 a_T}{1 + (\lambda_0 a_T \dot{\gamma})^{1-n}} \quad , \tag{3}$$

where η_0 is the viscosity at low shear rates (i.e., in the Newtonian plateau) measured at the (arbitrary) reference temperature T_0; λ_0 is a characteristic time, associated to the transition between Newtonian and pseudoplastic

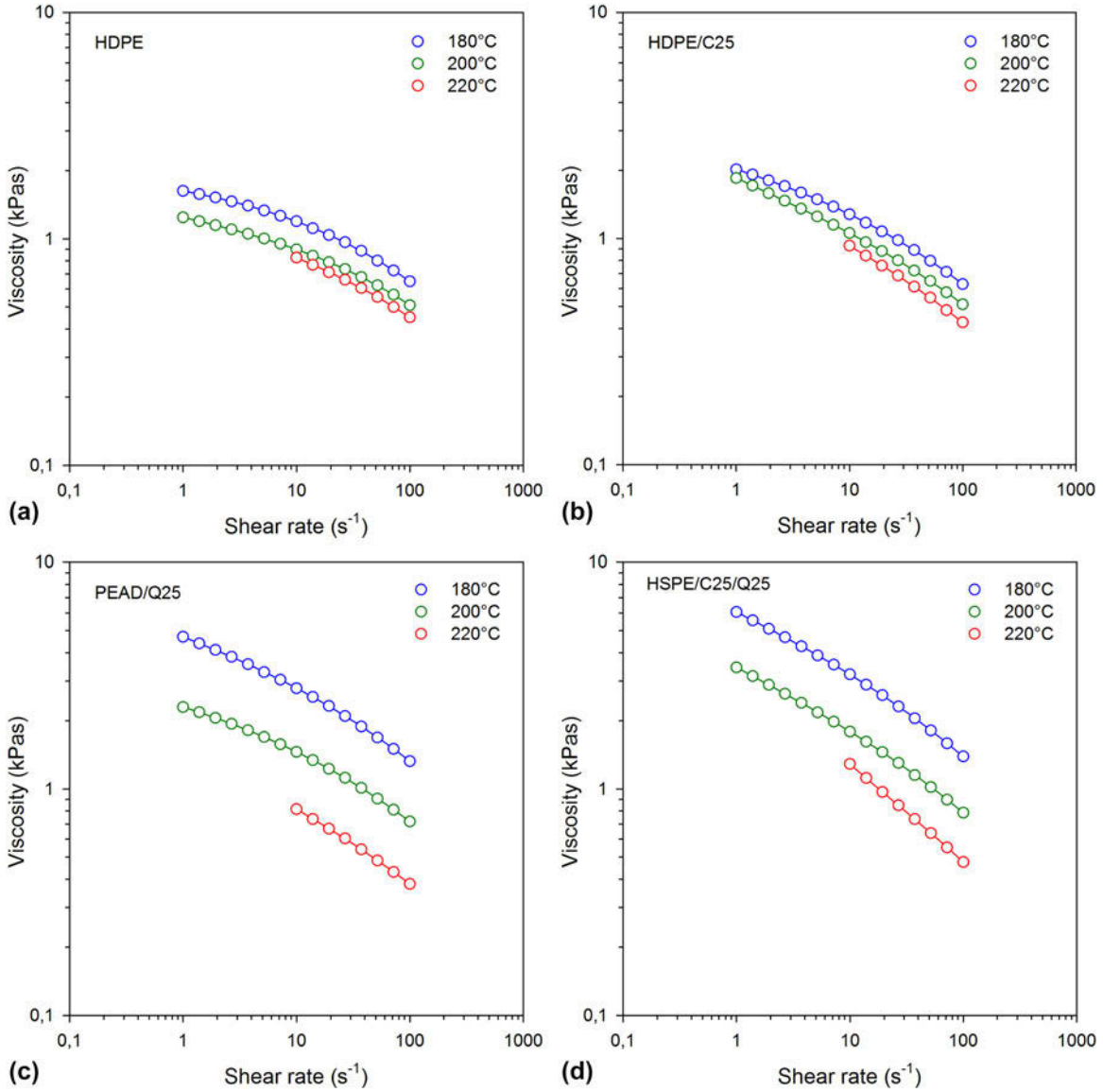

FIG. 4. Viscosity as function of shear rate at several temperatures, for neat HDPE (a), HDPE/25% PE-*g*-MA blend (b), and HDPE/chitosan compounds with 25% filler, without compatibilization (c) and with 25% PE-*g*-MA compatibilizer (d). Logarithmic scales.

behavior, measured at the same reference temperature T_0; n is the pseudoplasticity index (power law index); and a_T is a thermal shift factor that accounts for the temperature dependence of the Newtonian viscosity and the characteristic time. Among the models proposed for the shift factor[63,64] a simple exponential relationship was chosen:

$$a_T = \exp\{-\beta_0(T - T_0)\} \quad , \tag{4}$$

where β_0 is an empirical coefficient (the temperature coefficient of the Newtonian viscosity) and T_0 is previously selected reference temperature. Equation (4) is an excellent approximation for temperatures not too far from the reference. Viscosity parameters η_0, λ_0, n, and β_0 may be obtained by linear regression of the experimental data.

For the compounds, viscosity was correlated directly using a power law expression:

TABLE II. Viscosity parameters (T_0 = 180 °C).

	Cross		Power Law	
Parameter	HDPE	HDPE/C25	HDPE/Q25	HDPE/C25/Q25
m_0 (kPa s^n)	(7.72)	(4.95)	5.04	6.47
η_0 (kPa s)	2.135	3.727	...	...
λ_0 (s)	0.059	0.508	...	...
n	0.546	0.592	0.73	0.68
β_0 ($°C^{-1}$)	0.013	0.015	0.020	0.022

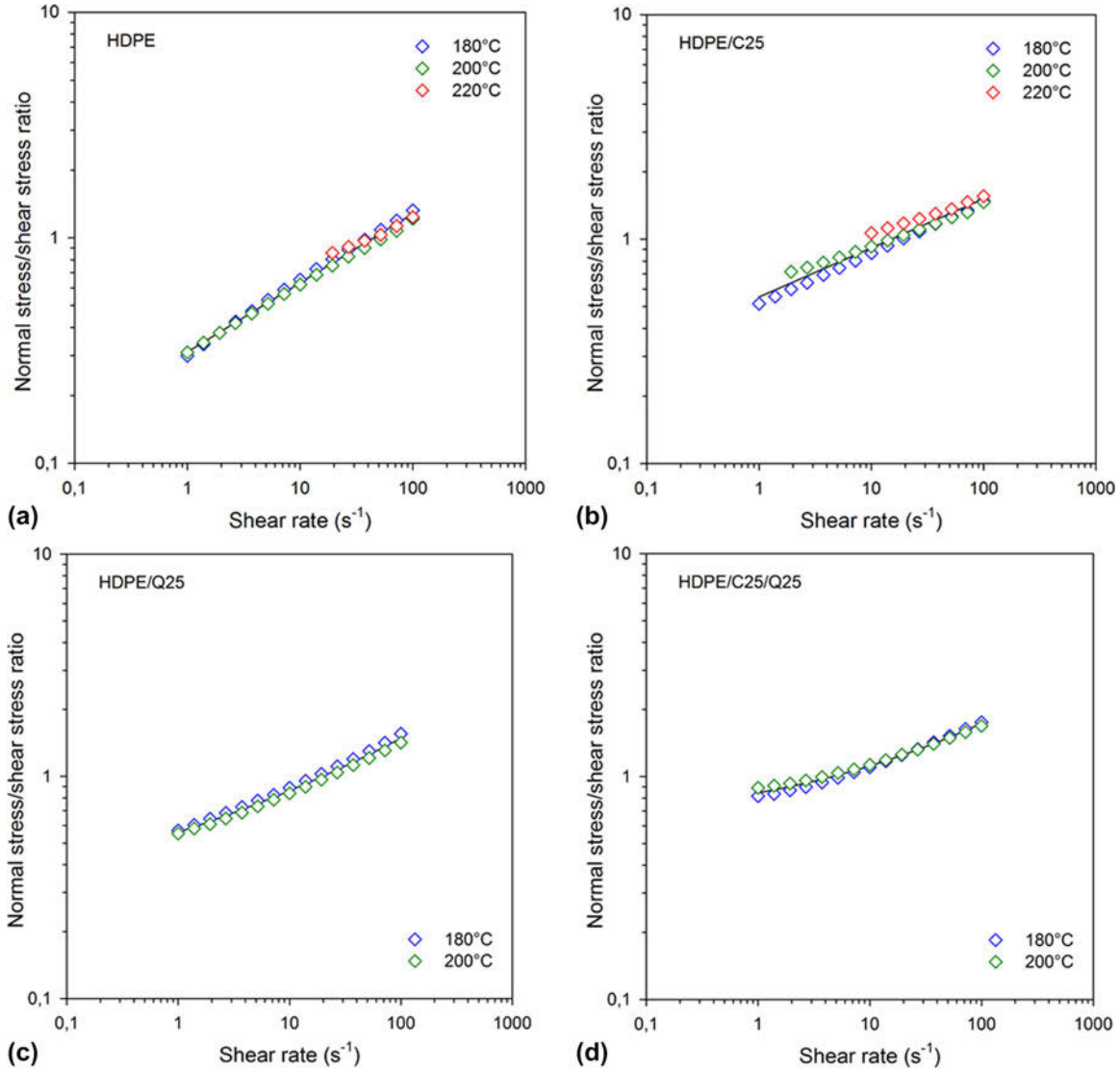

FIG. 5. Normal to shear stress ratio as function of shear rate at several temperatures, for neat HDPE (a), HDPE/25% PE-*g*-MA blend (b), and HDPE/chitosan compounds with 25% filler, without compatibilization (c) and with 25% PE-*g*-MA compatibilizer (d). Logarithmic scales.

$$\eta(\dot{\gamma}, T) = m_0 a_T \dot{\gamma}^{n-1} \quad , \tag{5}$$

where m_0 is the so-called *consistency* of the material measured at the reference temperature T_0 and n is the pseudoplasticity index. The shift factor a_T is now:

$$a_T = \exp\{-n\beta_0(T - T_0)\} \quad , \tag{6}$$

where $n\beta_0$ is the temperature coefficient of the Newtonian viscosity in the power-law zone; the parameter β_0 corresponds to the (hypothetical) Newtonian plateau.

Estimated viscosity parameters for systems are collected in Table II. Consistency for the unfilled samples was computed from Cross parameters as $m_0 = \eta_0 \lambda_0^{n-1}$.

Molten polymers and polymeric compounds are viscoelastic liquids. The elastic characteristics of the melt may be estimated from shear moduli using a useful, empirical correlation reported by Laun,[60,65,66] the equivalent of the Cox–Merz rule for the elastic components of the viscoelastic response. The first normal stress coefficient Ψ_1 is given, as a function of shear rate as:

$$\Psi_1(\dot{\gamma}) \approx \frac{2G'(\omega)}{\omega^2}\left[1 + \left(\frac{G'(\omega)}{G''(\omega)}\right)^2\right]^{0.7}_{\omega=\dot{\gamma}} \quad . \tag{7}$$

A measure of the relative importance of elastic characteristics of the melt—compared with its viscous characteristics—is the ratio of normal to shear stresses[64]:

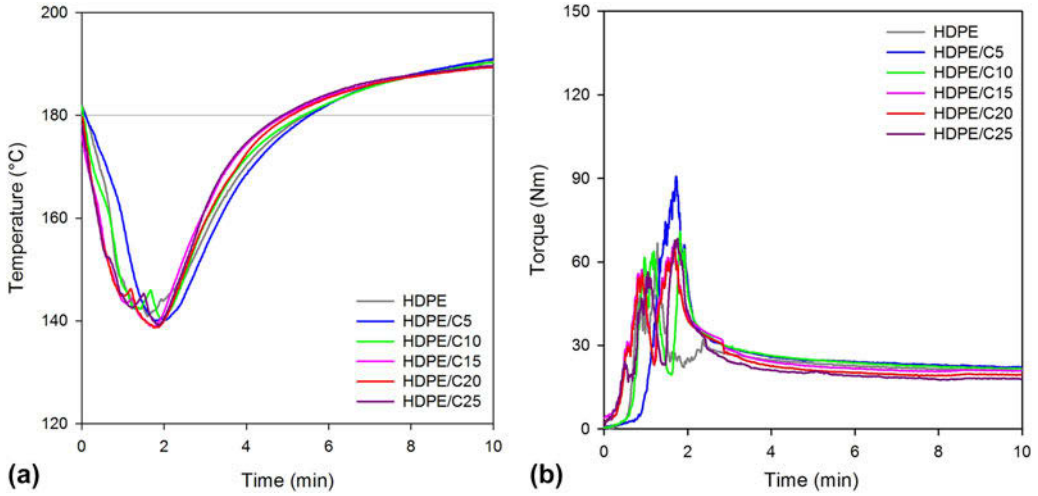

FIG. 6. Temperature (a) and torque (b) as functions of time during processing of HDPE and HDPE/PE-*g*-MA blends in the laboratory internal mixer.

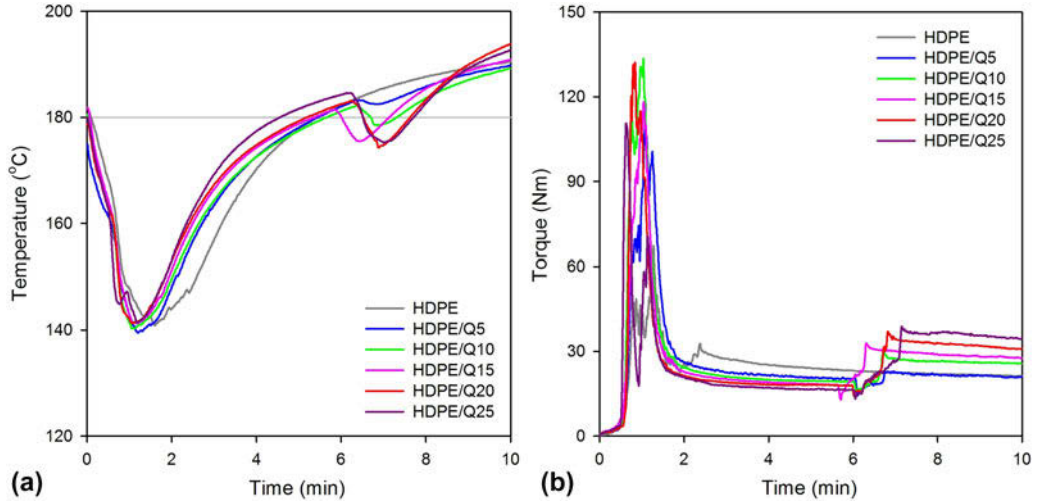

FIG. 7. Temperature (a) and torque (b) as functions of time during processing of HDPE and HDPE/chitosan compounds in the laboratory internal mixer; filler added at (approximately) 6 min processing time.

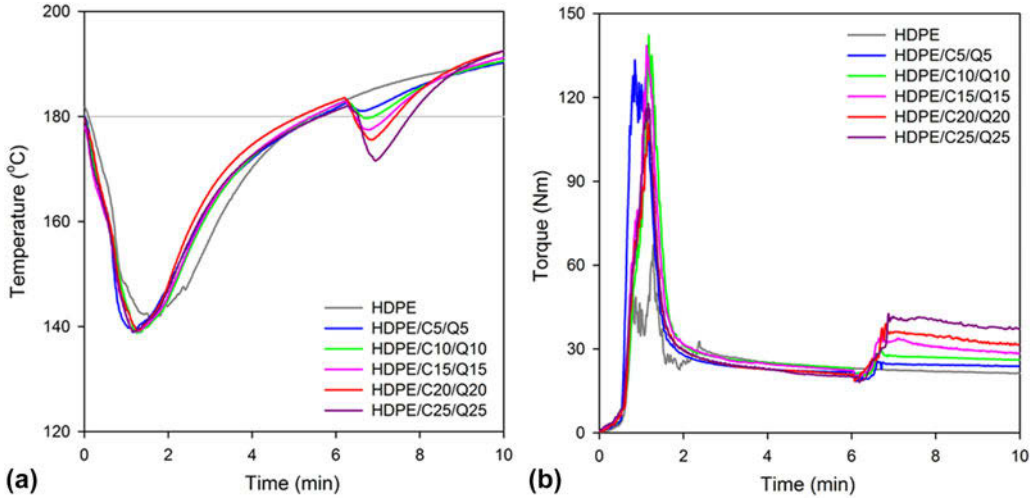

FIG. 8. Temperature (a) and torque (b) as functions of time during processing of HDPE and compatibilized HDPE/chitosan compounds in the laboratory internal mixer; filler added at (approximately) 6 min processing time.

$$S = \frac{N_1}{\tau} = \frac{\Psi_1 \dot{\gamma}}{\eta} \quad , \tag{8}$$

where N_1 is the first difference of normal stresses and τ is shear stress. From Eqs. (8) and (7) the stress ratio may be estimated in terms of shear moduli ratio G'/G'':

$$S \approx 2\frac{G'}{G''}\left[1 + \left(\frac{G'}{G''}\right)^2\right]^{0.2} \quad . \tag{9}$$

The stress ratio is shown in Fig. 5 as a function of shear rate for the systems studied.

Melts with $S \ll 1$ behave as purely viscous (Newtonian) fluids. In the present case, for the material, equipment, and processing conditions used in the tests, with shear rates in the range 10–100 s^{-1},[67] melts behave as typical viscoelastic fluids, and neither viscous nor elastic characteristics could be neglected. Flows in processing chamber of mixer and extruders are mostly shear flows and under these conditions viscoelasticity manifest itself as a pseudoplastic (non Newtonian) viscosity. Approximate global flow models in the processing chamber may be modeled without considering the elastic response in itself.

However, mixing during processing in batch and continuous equipment takes place predominantly in the gap between rotor wing tips and chamber walls, and in the neighboring wedge-like regions,[68] with high shear stresses and significant extensional components in the flow. The elastic characteristics of melt should be taken into consideration to model the mixing process.

C. Torque rheometry

Plots of temperature and torque versus time during processing of all systems tested are shown in Figs. 6–8.

TABLE III. Average terminal melt temperature, raw torque, and torque @ 180 °C.

Sistema	$\bar{T}$ (°C)	$\bar{Z}^{72}$ (N m)	$\overline{Z^*}$ (N m)
HDPE	189.9 ± 0.3	20.9 ± 0.1	23.11 ± 0.07
HDPE/C5	190.2 ± 0.4	22.3 ± 0.2	24.68 ± 0.13
HDPE/C10	189.7 ± 0.4	21.7 ± 0.1	23.95 ± 0.08
HDPE/C15	189.0 ± 0.2	21.0 ± 0.1	22.99 ± 0.06
HDPE/C20	189.0 ± 0.3	19.5 ± 0.1	21.36 ± 0.06
HDPE/C25	189.3 ± 0.3	18.0 ± 0.1	19.80 ± 0.08
HDPE/Q5	189.0 ± 0.5	21.1 ± 0.3	23.04 ± 0.20
HDPE/Q10	188.2 ± 0.6	25.9 ± 0.1	28.08 ± 0.11
HDPE/Q15	189.9 ± 0.6	28.0 ± 0.2	30.86 ± 0.16
HDPE/Q20	192.0 ± 1.1	31.3 ± 0.4	35.30 ± 0.09
HDPE/Q25	191.1 ± 1.0	35.0 ± 0.4	39.07 ± 0.20
HDPE/C5/Q5	189.4 ± 0.5	23.9 ± 0.1	26.27 ± 0.08
HDPE/C10/Q10	189.7 ± 0.6	26.3 ± 0.1	28.93 ± 0.07
HDPE/C15/Q15	190.1 ± 0.7	28.9 ± 0.3	31.97 ± 0.18
HDPE/C20/Q20	191.3 ± 0.8	32.0 ± 0.3	35.80 ± 0.19
HDPE/C25/Q25	191.0 ± 0.9	37.5 ± 0.3	41.90 ± 0.32

Torque is directly proportional to the rate of mechanical energy dissipation inside the processing chamber. The initial torque peak corresponds to dissipation by friction and plastic deformation in the particulate solids. Mechanical energy, dissipated as heat, increases the temperature and results in the melting of the polymer matrix; torque drops as viscous energy dissipation mechanisms (less efficient than dissipation mechanisms in compact particulate solids) are engaged.[67,69]

Plots show that the polymer matrix is substantially molten after 3–4 min processing time. For neat HDPE and HDPE/PE-*g*-MA blends (Fig. 6) melt temperate increases and torque decreases with time; for the compounds (Figs. 7 and 8), after filler addition at 6 min processing time, the same effects—more pronounced—are observed. Analysis of the torque–temperature–time relationships during the last stage of

TABLE IV. Corrected terminal torque differences.

C/Q	$Z^*_{PC} - Z^*_P$		$Z^*_{PQ} - Z^*_P$		$Z^*_{PCQ} - Z^*_{PC}$		$Z^*_{PCQ} - Z^*_{PQ}$	
5	1.6	(7%)	−0.1	...	1.6	(6%)	3.2	(14%)
10	0.8	(4%)	5.0	(22%)	5.0	(21%)	0.9	(3%)
15	−0.1	...	7.8	(36%)	9.0	(39%)	1.1	(4%)
20	−1.8	(−8%)	12.2	(53%)	14.4	(68%)	0.5	(1.4%)
25	−3.3	(−14%)	16.0	(69%)	22.1	(113%)	2.8	(7%)

(Torques in N m).

processing in internal mixers (processing of molten materials) follows the same methods discussed elsewhere[70,71] based on the proportionality of torque (Z) and viscosity (η) in tests performed at constant rotor speed:

$$Z \approx k\eta \quad . \tag{10}$$

In the present case, melt viscosity depends on shear rate, temperature, molar mass, and filler content. However, in first approximation, mean shear rate depends only on rotor speed, and since all tests were performed at the same rpm, dependence on shear rate may be embedded in the proportionality constant of Eq. (10). Moreover, for a single test—at given filler concentration—the torque depends only on temperature and molar mass that may change with time due to degradation of the matrix. To isolate the dependence of torque on molar mass, and verify if there were in fact a significant degradation of the polymers, a "corrected" torque Z^* is defined as the torque that would be observed at a (constant in time) reference temperature T^*. Taking advantage of the known dependence of the viscosity with temperature, Eq. (11):

$$Z^* = Z \exp\{n\beta_0(T - T^*)\} \quad , \tag{11}$$

where Z and T are the experimental values of torque and temperature during the last stage of processing. The index of pseudoplasticity n and temperature coefficient β_0 are taken from Table II, and assumed to be independent of the filler and/or compatibilizer concentration. Results (not shown here) reveal that the mild decrease of torque with time could be accounted by the increase in melt temperature. Consequently, polymer degradation at the processing conditions tested may be disregarded.

Of particular interest are the terminal values of torque and temperature, computed as the average between 9 and 10 min processing time with a reference temperature $T^* = 180$ °C, collected in Table III.

Blends HDPE/PE-*g*-MA show a reduction of torque with the increase of compatibilizer content, perhaps due to its lower viscosity. HDPE/chitosan compounds show a significant increase in torque with the increase of filler content. The increase is even greater in compatibilized compounds. Torque differences shown in Table IV allow a quantitative appraisal of the effect of filler and compatibilizer. The same results are presented graphically in Fig. 9.

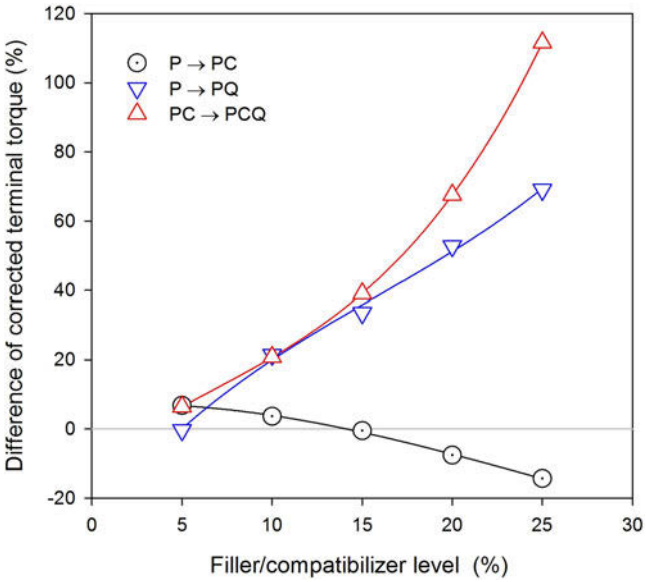

FIG. 9. Corrected terminal torque comparison, showing the effect compatibilizer, (a) and torque (b) as functions of time during processing of HDPE and compatibilizer (P → PC), filler (P → PQ), and compatibilizer plus filler (PC → PCQ).

The first column of Table IV ($Z^*_{PC} - Z^*_P$) compares the corrected terminal torque processing HDPE/PE-*g*-MA blends with that obtained with neat HDPE. Torque (i.e., melt viscosity) in the blend is higher for less than 15% compatibilizer and lower for more than 15%. The second column ($Z^*_{PQ} - Z^*_P$) considers the effect of chitosan addition to HDPE without compatibilizer. Torque increases steadily with filler concentration, up to a 69% increase for the compound with 25% filler. The effect of chitosan content is greater in compatibilized compounds with 15% or more filler, up to 113% for the compound with 25% filler compared with its matrix (the blend in this case), as shown in the third column ($Z^*_{PCQ} - Z^*_{PC}$). At lower filler levels, the compatibilizer may play an internal lubricating role, facilitating the orientation and distribution of filler particles in flow, and resulting in a decrease in the viscosity.[73] At higher filler

levels it is clear that the PE-*g*-MA affected the microstructure of the compounds, possibly increasing matrix–filler interactions and acting as an effective compatibilizer.

The viscosity of polymer compounds is usually correlated in terms of volumetric fraction of filler ϕ estimated at processing conditions as:

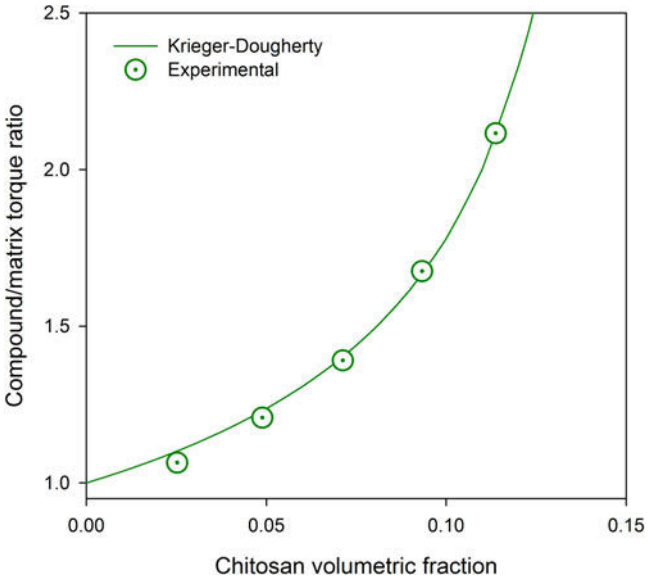

FIG. 10. Compatibilized compound (HDPE/PE-*g*-MA/chitosan) to matrix (HDPE/PE-*g*-MA) terminal corrected torque ratio as a function of the volumetric fraction of filler (chitosan). Line corresponds to Krieger–Dougherty model, Eq. (13).

$$\phi = \left(1 + \frac{1-w}{w} \cdot \frac{\rho_Q}{\rho_P}\right)^{-1} \quad , \tag{12}$$

where w is the mass fraction of filler and ρ_Q, ρ_Q, are the filler (Q) and matrix (P) densities, respectively, measured at the processing temperature (around 190 °C in the present case).

Several models were proposed for the dependence of the viscosity of concentrated suspensions on the filler's concentration.[63,74,75] The semi empirical model of Ref. 76 is one of the most commonly used to correlate experimental results in systems without specific particle–particle and particle–matrix interactions. Considering that—in the absence of degradation—corrected torque is a function of the filler content only, the model could be expressed as:

$$Z^*_{\text{compound}} = Z^*_{\text{matrix}} \left(1 - \frac{\phi_{\text{filler}}}{\phi_{\text{m}}}\right)^{-\alpha\phi_{\text{m}}} \quad , \tag{13}$$

where the volumetric fraction of the filler is estimated from Eq. (12), parameters ϕ_m and α are obtained by fitting Eq. (13) to experimental data.

Parameter ϕ_m is associated to the maximum filler concentration in a fluid system. Equation (13) predicts $Z^*_{\text{compound}} \rightarrow \infty$ for $\phi_{\text{filler}} \rightarrow \phi_m$; for this reason, ϕ_m corresponds to the percolation limit of the suspension. Parameter α is often called the *intrinsic viscosity* of the

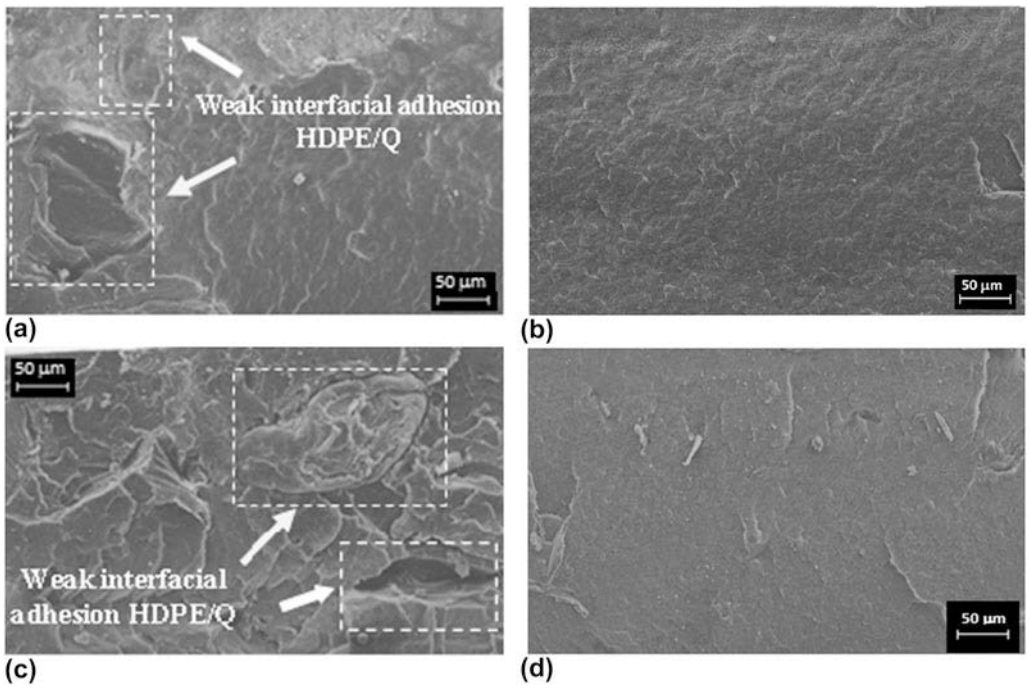

FIG. 11. SEM images for HDPE/chitosan compounds, (a) HDPE/Q5, (b) HDPE/C5/Q5, (c) HDPE/Q10 and (d) HDPE/C10/Q10. Scale bars indicated.

compound under processing conditions, where the molten polymer matrix acts as a "solvent" of the particulate filler; α is strongly affected by the shape of the suspended particles.

The corrected terminal torque results for the compatibilized HDPE/chitosan compounds were fitted to the Krieger–Dougherty equation, considering as the matrix the HDPE/PE-*g*-MA blend with the same compatibilizer content as the compound. Nonlinear regression gave the following values for the parameters:

$$\phi_m = 0.15 \pm 0.01$$

$$\alpha = 3.50 \pm 0.15 \quad .$$

For HDPE/chitosan compounds at 190 °C, the maximum volumetric fraction $\phi_m = 0.15$ corresponds to a mass fraction of 26% approximately. The high intrinsic viscosity observed ($\alpha > 2$) is consistent with the isometric morphology of the chitosan.[74] Fig. 10 shows the excellent fit obtained.

D. Scanning electron microscopy

Figure 11 presents SEM images for HDPE/Q and HDPE/C/Q compounds, these images show the effects of 5 and 10% of chitosan in HDPE matrix and the influence of adding the PE-*g*-MA compatibilizer in the HDPE/Q compounds.

Smooth surfaces are observable in HDPE/Q compounds [Figs. 11(a) and 11(c)] suggesting brittle fracture with low energy absorption, and possibly some plastic deformation. Upon addition of PE-*g*-MA the images show more homogeneous surfaces, with no segregation [Figs. 11(b) and 11(d)]. The formation of rough surfaces may be associated with higher energy absorption for fracturing.

It is possible that PE-*g*-MA contributed to higher interfacial adhesion between HDPE and chitosan and to a better dispersion of chitosan particles into the HDPE matrix.

IV. CONCLUSIONS

Chitosan can be mixed with high-density polyethylene (HDPE) and maleated polyethylene (PE-*g*-MA) to obtain composites prepared by melt compounding technique in a laboratory internal mixer. The rheological behavior of the prepared composites was investigated by a parallel plate rheometer and laboratory internal mixer to understand the effects of both chitosan and PE-*g*-MA (compatibilizer) on rheological behavior of the composites. The results indicated that the presence of chitosan increases the complex viscosity, loss modulus, storage modulus and the torque (i.e., melt viscosity), and the combination chitosan/compatibilizer has a similar, if slighter, effect. At higher filler levels (greater than 15%) the PE-*g*-MA affected the rheological behavior of the compounds, possibly increasing matrix–filler interactions and acting as an effective compatibilizer.

ACKNOWLEDGMENTS

The authors are grateful to the Braskem and Chemtura for the donation of the polyethylene resin and maleated polyethylene, and to the Conselho Nacional de Pesquisa (CNPq—Brazil), Grant # 478968/2013-2, Coordenação de Aperfeiçoamento de Pessoal de Nível Superior (CAPES—Brazil) and Fundação de Amparo à Ciência e Tecnologia do Estado de Pernambuco (FACEPE—Brazil), DCR-0009-3.03/12, for financial support.

REFERENCES

1. A. Peacock: *Handbook of Polyethylene: Structures: Properties, and Applications* (CRC Press, New York, 2000).
2. C. Vasile and M. Pascu: *Practical Guide to Polyethylene* (Rapra Technology Limited, Shawbury, 2005).
3. D.B. Malpass: *Introduction to Industrial Polyethylene: Properties, Catalysts, and Processes* (John Wiley & Sons, Hoboken, 2010).
4. S. Bonhomme, A. Cuer, A. Delort, J. Lemaire, M. Sancelme, and G. Scott: Environmental biodegradation of polyethylene. *Polym. Degrad. Stab.* **81**(3), 441 (2003).
5. G. Scott: *Polymers and the Environment* (Royal Society of Chemistry, Cambridge, 1999).
6. G. Swift and D. Wiles: Biodegradable and degradable polymers and plastics in landfill sites. In *Encyclopedia of Polymer Science and Technology*, J.I. Kroschwitz, ed. (John Wiley & Sons., Hoboken, 2004).
7. M. Sudhakar, M. Doble, P.S. Murthy, and R. Venkatesan: Marine microbe-mediated biodegradation of low-and high-density polyethylenes. *Int. Biodeterior. Biodegrad.* **61**(3), 203 (2008).
8. T. Ojeda, A. Freitas, K. Birck, E. Dalmolin, R. Jacques, F. Bento, and F. Camargo: Degradability of linear polyolefins under natural weathering. *Polym. Degrad. Stab.* **96**(4), 703 (2011).
9. R.A. Gross and B. Kalra: Biodegradable polymers for the environment. *Science* **297**(5582), 803 (2002).
10. Y.V. Kissin: *Polyethylene: End-use Properties and Their Physical Meaning* (Carl Hanser Verlag GmbH Co KG, Cincinnati, 2012).
11. M. Tolinski: *Additives for Polyolefins: Getting the Most Out of Polypropylene, Polyethylene and TPO* (William Andrew, Oxford, 2015).
12. S. Husseinsyah, A.N. Azmin, and H. Ismail: Effect of maleic anhydride-grafted-polyethylene (MAPE) and silane on properties of recycled polyethylene/chitosan biocomposites. *Polym.-Plast. Technol. Eng.* **52**(2), 168 (2013).
13. Y. Orhan, J. Hrenovic, and H. Buyukgungor: Biodegradation of plastic compost bags under controlled soil conditions. *Acta Chim. Slov.* **51**(3), 579 (2004).
14. S.Z. Rogovina, K.V. Aleksanyan, D.D. Novikov, E.V. Prut, and A.V. Rebrov: Synthesis and investigation of polyethylene blends with natural polysaccharides and their derivatives. *Polym. Sci., Ser. A* **51**(5), 554 (2009).
15. S.Z. Rogovina, C.V. Alexanyan, and E.V. Prut: Biodegradable blends based on chitin and chitosan: Production, structure, and properties. *J. Appl. Polym. Sci.* **121**(3), 1850 (2011).
16. H. Ismail, S.M. Shaari, and N. Othman: The effect of chitosan loading on the curing characteristics, mechanical and morphological

properties of chitosan-filled natural rubber (NR), epoxidised natural rubber (ENR) and styrene-butadiene rubber (SBR) compounds. *Polym. Test.* **30**(7), 784 (2011).
17. V. Correlo, L. Boesel, M. Bhattacharya, J. Mano, N. Neves, and R. Reis: Properties of melt processed chitosan and aliphatic polyester blends. *Mater. Sci. Eng., A* **403**(1), 57 (2005).
18. O. Ermolovich and A. Makarevich: Effect of compatibilizer additives on the technological and performance characteristics of biodegradable materials based on starch-filled polyethylene. *Russ. J. Appl. Chem.* **79**(9), 1526 (2006).
19. D. Raghavan and A. Emekalam: Characterization of starch/polyethylene and starch/polyethylene/poly (lactic acid) composites. *Polym. Degrad. Stab.* **72**(3), 509 (2001).
20. C-S. Wu: A comparison of the structure, thermal properties, and biodegradability of polycaprolactone/chitosan and acrylic acid grafted polycaprolactone/chitosan. *Polymer* **46**(1), 147 (2005).
21. S. Husseinsyah, F. Amri, K. Husin, and H. Ismail: Mechanical and thermal properties of chitosan-filled polypropylene composites: The effect of acrylic acid. *J. Vinyl Addit. Technol.* **17**(2), 125 (2011).
22. H. Salmah, A. Faisal, and H. Kamarudin: Chemical modification of chitosan-filled polypropylene (PP) composites: The effect of 3-aminopropyltriethoxysilane on mechanical and thermal properties. *Int. J. Polym. Mater.* **60**(7), 429 (2011).
23. H. Salmah, F. Amri, and H. Kamarudin: Properties of chitosan-filled polypropylene (PP) composites: The effect of acetic acid. *Polym.-Plast. Technol. Eng.* **51**(1), 86 (2012).
24. F. Amri, S. Husseinsyah, and K. Hussin: Mechanical, morphological and thermal properties of chitosan filled polypropylene composites: The effect of binary modifying agents. *Composites, Part A* **46**, 89 (2013).
25. O. Agboh and Y. Qin: Chitin and chitosan fibers. *Polym. Adv. Technol.* **8**(6), 355 (1997).
26. K. Chang, Y-S. Lin, and R. Chen: The effect of chitosan on the gel properties of tofu (soybean curd). *J. Food Eng.* **57**(4), 315 (2003).
27. P. Dutta, S. Tripathi, G. Mehrotra, and J. Dutta: Perspectives for chitosan based antimicrobial films in food applications. *Food Chem.* **114**(4), 1173 (2009).
28. B. Krajewska: Application of chitin-and chitosan-based materials for enzyme immobilizations: A review. *Enzyme Microb. Technol.* **35**(2), 126 (2004).
29. M.G. Peter: Applications and environmental aspects of chitin and chitosan. *J. Macromol. Sci., Part A: Pure Appl. Chem.* **32**(4), 629 (1995).
30. C. Pillai, W. Paul, and C.P. Sharma: Chitin and chitosan polymers: Chemistry, solubility and fiber formation. *Prog. Polym. Sci.* **34**(7), 641 (2009).
31. K.H. Prashanth and R. Tharanathan: Chitin/chitosan: Modifications and their unlimited application potential—An overview. *Trends Food Sci. Technol.* **18**(3), 117 (2007).
32. E.I. Rabea, M.E.-T. Badawy, C.V. Stevens, G. Smagghe, and W. Steurbaut: Chitosan as antimicrobial agent: Applications and mode of action. *Biomacromolecules* **4**(6), 1457 (2003).
33. S.A. Agnihotri, N.N. Mallikarjuna, and T.M. Aminabhavi: Recent advances on chitosan-based micro-and nanoparticles in drug delivery. *J. Controlled Release* **100**(1), 5 (2004).
34. J-K.F. Suh and H.W. Matthew: Application of chitosan-based polysaccharide biomaterials in cartilage tissue engineering: A review. *Biomaterials* **21**(24), 2589 (2000).
35. K.V. Reesha, S.K. Panda, J. Bindu, and T.O. Varghese: Development and characterization of an LDPE/chitosan composite antimicrobial film for chilled fish storage. *Int. J. Biol. Macromol.* **79**, 934 (2015).
36. S. Khoramnejadian: Kinetic study of biodegradation of linear low density polyethylene/chitosan. *Adv. Environ. Biol.*, **5**(10), 3050 (2011).
37. A. Martínez-Camacho, M. Cortez-Rocha, A. Graciano-Verdugo, F. Rodríguez-Félix, M. Castillo-Ortega, A. Burgos-Hernández, J. Ezquerra-Brauer, and M. Plascencia-Jatomea: Extruded films of blended chitosan, low density polyethylene and ethylene acrylic acid. *Carbohydr. Polym.* **91**(2), 666 (2013).
38. S. Mir, T. Yasin, P.J. Halley, H.M. Siddiqi, and T. Nicholson: Thermal, rheological, mechanical and morphological behavior of HDPE/chitosan blend. *Carbohydr. Polym.* **83**(2), 414 (2011).
39. A.O. Ogah, J.N. Afiukwa, and A.A. Nduji: Characterization and comparison of rheological properties of agro fiber filled high-density polyethylene bio-composites. *Open J. Polym. Chem.* **04**(01), 12 (2014).
40. S.I. Park, K.S. Marsh, and P. Dawson: Application of chitosan-incorporated LDPE film to sliced fresh red meats for shelf life extension. *Meat Sci.* **85**(3), 493 (2010).
41. J. Quiroz-Castillo, D. Rodríguez-Félix, H. Grijalva-Monteverde, T. del Castillo-Castro, M. Plascencia-Jatomea, F. Rodríguez-Félix, and P. Herrera-Franco: Preparation of extruded polyethylene/chitosan blends compatibilized with polyethylene-graft-maleic anhydride. *Carbohydr. Polym.* **101**, 1094 (2014).
42. D.E. Rodríguez-Félix, J.M. Quiroz-Castillo, H. Grijalva-Monteverde, T. Castillo-Castro, S.E. Burruel-Ibarra, F. Rodríguez-Félix, T. Madera-Santana, R.E. Cabanillas, and P.J. Herrera-Franco: Degradability of extruded polyethylene/chitosan blends compatibilized with polyethylene-*graft*-maleic anhydride under natural weathering. *J. Appl. Polym. Sci.* **131**(22), 41045 (2014).
43. H. Salmah and A.N. Azieyanti: Properties of recycled polyethylene/chitosan composites: The effect of polyethylene-graft-maleic anhydride. *J. Reinf. Plast. Compos.* **30**(3), 195 (2010).
44. M. Sunilkumar, T. Francis, E.T. Thachil, and A. Sujith: Low density polyethylene–chitosan composites: A study based on biodegradation. *Chem. Eng. J.* **204–206**, 114 (2012).
45. M. Sunilkumar, A.A. Gafoor, A. Anas, A.P. Haseena, and A. Sujith: Dielectric properties: A gateway to antibacterial assay—A case study of low-density polyethylene/chitosan composite films. *Polym. J.* **46**(7), 422 (2014).
46. C. Vasile, R. Darie, A. Sdrobiş, E. Paslaru, G. Pricope, A. Baklavaridis, S. Munteanu, and I. Zuburtikudis: Effectiveness of chitosan as antimicrobial agent in LDPE/CS composite films as minced poultry meat packaging materials. *Cellul. Chem. Technol.* **48**(3–4), 325 (2014).
47. C. Vasile, R.N. Darie, C.N. Cheaburu-Yilmaz, G-M. Pricope, M. Bračič, D. Pamfil, G.E. Hitruc, and D. Duraccio: Low density polyethylene–chitosan composites. *Composites, Part B* **55**, 314 (2013).
48. H-s. Wang, D. Chen, and C-z. Chuai: Mechanical and barrier properties of LLDPE/chitosan blown films for packaging. *Packag. Technol. Sci.* **28**(10), 915 (2015).
49. H.Z. Zhang, Z.C. He, G.H. Liu, and Y.Z. Qiao: Properties of different chitosan/low-density polyethylene antibacterial plastics. *J. Appl. Polym. Sci.* **113**(3), 2018 (2009).
50. P.S. Lima, C.F. Guedes, D.L.A.C.S. Andrade, E.L. Canedo, and S.M.L. Silva: High density polyethylene/chitosan compounds: Effect of load level on thermal and mechanical properties. In *2nd Brazilian Conference on Composite Materials—BCCM2* (São José dos Campos, 2014).
51. Braskem: High Density Polyethylene JV-060U Technical Data Sheet, Revision 8 (São Paulo, 2015).
52. D. Walsh and P. Zoller: *Standard Pressure Volume Temperature Data for Polymers* (CRC Press, Lancaster, 1995).
53. T. Yui, K. Imada, K. Okuyama, Y. Obata, K. Suzuki, and K. Ogawa: Molecular and crystal structure of the anhydrous form of chitosan. *Macromolecules* **27**(26), 7601 (1994).

54. J. Li, J. Revol, E. Naranjo, and R. Marchessault: Effect of electrostatic interaction on phase separation behaviour of chitin crystallite suspensions. *Int. J. Biol. Macromol.* **18**(3), 177 (1996).
55. C.P.F. Santos and S.L.A. Dantas: Avaliação de uma amostra de quitosana comercial para uso no tratamento de efluentes têxteis. Presented at the *48th Brazilian Chemistry Meeting* (Rio de Janeiro, 2008).
56. Addivant: Polybond 3009 Technical Information [www.addivant.com] (Danbury, 2013).
57. H. Moussout, H. Ahlafi, M. Aazza, and M. Bourakhouadar: Kinetics and mechanism of the thermal degradation of biopolymers chitin and chitosan using thermogravimetric analysis. *Polym. Degrad. Stab.* **130**, 1 (2016).
58. W. Cox and E. Merz: Correlation of dynamic and steady-flow viscosities. *J. Polym. Sci., Part A-2: Polym. Phys.* **28**, 619 (1958).
59. J.M. Dealy and R.G. Larson: *Structure and Rheology of Molten Polymers* (Hanser Publishers, Munich, 2006).
60. H.H. Winter: Three views of viscoelasticity for Cox–Merz materials. *Rheol. Acta* **48**(3), 241 (2009).
61. W. Gleissle and B. Hochstein: Validity of the Cox–Merz rule for concentrated suspensions. *J. Rheol.* **47**(4), 897 (2003).
62. M.M. Cross: Rheology of non-Newtonian fluids: A new flow equation for pseudoplastic systems. *J. Colloid Sci.* **20**(5), 417 (1965).
63. P.J. Carreau, D. De Kee, and R.P. Chhabra: *Rheology of Polymeric Systems: Principles and Applications* (Hanser Publishers, Munich, 1997).
64. R.B. Bird, R.C. Armstrong, and O. Hassager: Dynamics of polymeric liquids. In *Fluid Mechanics*, Vol. 1, 2nd ed. (John Wiley & Sons, New York, 1987).
65. H.M. Laun: Prediction of elastic strains of polymer melts in shear and elongation. *J. Rheol.* **30**(3), 459 (1986).
66. V. Sharma and G.H. McKinley: An intriguing empirical rule for computing the first normal stress difference from steady shear viscosity data for concentrated polymer solutions and melts. *Rheol. Acta* **51**(6), 487 (2012).
67. T.S. Alves, J.E.S. Neto, S.M.L. Silva, L.H. Carvalho, and E.L. Canedo: Process simulation of laboratory internal mixers. *Polym. Test.* **50**, 94 (2016).
68. E.L. Canedo and L.N. Valsamis: *Continuous Mixers, in Mixing and Compounding of Polymers*, 2nd ed., I. Manas-Zloczower, ed. (Hanser Publishers, Munich, 2009); p. 1081.
69. M.D. Wetzel and C.K. Shih: Experimental simulation with a simple mixer and real material. In *Mixing and Compounding of Polymers*, I. Manas-Zloczower, ed. (Hanser Publishers, Munich, 2009); p. 479.
70. A.R.M. Costa, T.G. Almeida, S.M.L. Silva, L.H. Carvalho, and E.L. Canedo: Chain extension in poly (butylene-adipate-terephthalate). Inline testing in a laboratory internal mixer. *Polym. Test.* **42**, 115 (2015).
71. A.A. Tavares, D.F. Silva, P.S. Lima, D.L. Andrade, S.M. Silva, and E.L. Canedo: Chain extension of virgin and recycled polyethylene terephthalate. *Polym. Test.* **50**, 26 (2016).
72. I. Aranaz, M. Mengíbar, R. Harris, I. Paños, B. Miralles, N. Acosta, G. Galed, and Á. Heras: Functional characterization of chitin and chitosan. *Curr. Chem. Biol.* **3**(2), 203 (2009).
73. V. Hristov and J. Vlachopoulos: Effects of polymer molecular weight and filler particle size on flow behavior of wood polymer composites. *Polym. Compos.* **29**(8), 831 (2008).
74. H.A. Barnes, J.F. Hutton, and K. Walters: *An Introduction to Rheology* (Elsevier, Amsterdam, 1989).
75. A.V. Shenoy: *Rheology of Filled Polymer Systems* (Springer Science & Business Media, Dordrecht, 1999).
76. I.M. Krieger and T.J. Dougherty: A mechanism for non-Newtonian flow in suspensions of rigid spheres. *Trans. Soc. Rheol.* **3**(1), 137 (1959).